FOORDITE SnNb₂O₆, A NEW MINERAL SPECIES, AND THE FOORDITE–THOREAULITE SERIES

PETR ČERNÝ

Department of Geological Sciences, University of Manitoba, Winnipeg, Manitoba R3T 2N2

ANDRÉ-MATHIEU FRANSOLET

Institut de Minéralogie, Université de Liège, B-4000 Liège, Belgique

T. SCOTT ERCIT

Mineral Sciences Division, National Museum of Natural Sciences, Ottawa, Ontario K1A 0M8

RON CHAPMAN

Department of Geological Sciences, University of Manitoba, Winnipeg, Manitoba R3T 2N2

ABSTRACT

The new mineral species *foordite* was identified in specimens previously described as thoreaulite from Lutsiro, Sebeya River, Rwanda and Punia, Zaire. The Lutsiro holotype is brownish yellow, with a greenish tint, has a yellowish white streak, vitreous to adamantine lustre and is not fluorescent. D_{meas} 6.73, D_{calc} 6.66 g/cm³, $H = 6$. Foordite is biaxial (+), $2V$ intermediate, $(\alpha + \beta + \gamma)/3 = 2.294$ (calc.), $\gamma - \alpha > 0.100$ (est.). The chemical composition of the holotype is SnO 25.4, PbO 6.0, Ta₂O₅ 28.7, Nb₂O₅ 40.1, total 100.2 wt.%, leading to the formula $(Sn_{0.87}Pb_{0.13})_{\Sigma1.00}(Nb_{1.40}Ta_{0.60})_{\Sigma2.00}O_6$, ideally SnNb₂O₆ ($Z = 4$). The X-ray powder pattern is close to that of thoreaulite. The unit-cell dimensions are a 17.093(3), b 4.877(1), c 5.558(1) Å, β 90.85(1)°, V 463.3 Å³, space group C2/c. The mineral is named after Dr. Eugene E. Foord, who predicted its existence. In the foordite SnNb₂O₆ – thoreaulite SnTa₂O₆ series, increasing Ta/(Ta + Nb) leads to an increase in D and a, and a decrease in b, c, and indices of refraction, whereas V and β remain virtually constant; these relationships are disturbed by the substitution of Pb and Sb. Crystal-chemical

and structural considerations lead to the conclusion that the proportion of Sn^{4+} is negligible. Foordite is expected to be a rare mineral in general, as well as in relation to thoreaulite. Stabilization of foordite requires low $f(O_2)$, low μ(Fe,Mn,Na,Ca,F), and low μ(Ta/Nb), an environment that is unusual during late stages of consolidation in granitic pegmatites.

Keywords: foordite, thoreaulite, tin, niobium, new mineral species, granitic pegmatite, Rwanda, Zaire.

SOMMAIRE

La foordite, nouvelle espèce minérale, a été identifiée dans des échantillons précédemment décrits comme thoreaulite et provenant de Lutsiro, le long de la rivière Sebeya (Ruanda), et de Punia (Zaïre). L'holotype de Lutsiro est jaune brunâtre avec une teinte verdâtre, possède une rayure blanc jaunâtre, un éclat vitreux à adamantin, et ne montre aucune fluorescence. D_{mes} 6.73; D_{calc} 6.66; dureté 6. Le minéral est biaxe (+), $2V$ moyen, $(\alpha + \beta + \gamma)/3 = 2.294$

(calc.), $\gamma-\alpha > 0.100$ (estimé). L'holotype contient SnO 25.4, PbO 6.0, Ta_2O_5 28.7, Nb_2O_5 40.1, total 100.2% (en poids), conduisant à la formule $(Sn_{0.87}Pb_{0.13})_{\Sigma 1.00}(Nb_{1.40}$ $Ta_{0.60})_{\Sigma 2.00}O_6$, ou, idéalement, $SnNb_2O_6$ ($Z = 4$). Le cliché de poudres, obtenu par diffraction X, est voisin de celui de la thoreaulite. Les paramètres de la maille sont: a 17.093(3), b 4.877(1), c 5.558(1) Å, β 90.85(1)°, V 463.3 Å³, groupe spatial $C2/c$. Le nom du minéral honore M. Eugene E. Foord, qui avait prévu son existence. Dans la série foordite $SnNb_2O_6$ – thoreaulite $SnTa_2O_6$, un accroissement de Ta/(Ta + Nb) provoque une augmentation de la densité, et une diminution de b, c, et des indices de réfraction, alors que V et β demeurent pratiquement constants; ces relations sont perturbées par la substitution de Pb et de Sb. Des considérations cristallochimiques et structurales permettent de conclure que la proportion de Sn^{4+} est négligeable. La foordite constitue un minéral rare en général, de même que vis-à-vis de la thoreaulite. Sa stabilisation requiert un $f(O_2)$, un $\mu(Fe,Mn,Na,Ca,F)$, et un $\mu(Ta,Nb)$ faibles, ce qui représente un environnement tout à fait inhabituel au cours des derniers stades de la mise en place des pegmatites granitiques.

Mots-clés: foordite, thoreaulite, étain, niobium, nouvelle espèce minérale, pegmatite granitique, Ruanda, Zaïre.

INTRODUCTION

The rare mineral *thoreaulite* was first described by Buttgenbach (1933) from the Manono pegmatite deposit in Zaire. The mineral, discovered later at a few additional localities, was assigned the formula $Sn^{4+}Ta_2O_7$ (Mélon 1935, Bailly 1942, Barsanov & Ginsburg 1946, Thoreau *et al.* 1950, Mélon & Toussaint 1950). The first structure-refinements were executed with this formula in mind, but were biased by the expectation of the seventh oxygen atom (Maksimova & Ilyukhin 1967, Mumme 1970). The dominant to exclusive presence of Sn^{2+} and the formula $Sn^{2+}Ta_2O_6$ were predicted on structural grounds (Graham & Thornber 1974, Maksimova *et al.* 1975), and were recently confirmed by Mössbauer spectroscopy (Nekrasov *et al.* 1982, 1984).

Thoreaulite from Lutsiro, Sebeya River, Rwanda was chemically analyzed by Thoreau *et al.* (1950) and was shown to have Nb/Ta (atomic) greater than 1. The above authors and, *i.a.*, Gorzhevskaya & Sidorenko (1974) and Nekrasov *et al.* (1982), concluded that the Lutsiro thoreaulite represents a Nb-rich member of an isomorphous series. However, the relatively high FeO content (1.98 wt.%) of the material analyzed by Thoreau *et al.* (1950) indicated contamination by about 15% of the associated Nb-rich columbite, which would significantly affect the Nb/Ta ratio. Consequently, Foord (1982) called both for further study of thoreaulite by microprobe techniques, and for a name for the Nb-dominant phase as a distinct species, should its natural occurrence be confirmed.

The present paper is the result of such a study,

which led to the establishment of $SnNb_2O_6$ as a new mineral, and to a better understanding of the natural members of the $SnNb_2O_6$–$SnTa_2O_6$ series. The new mineral species was named *foordite* (pronounced FŌR·DAIT) in honor of Dr. E.E. Foord, a distinguished student of granitic pegmatites and particularly their complex Nb-Ta-bearing oxide minerals. The new mineral and its name were approved by the Commission on New Minerals and Mineral Names, International Mineralogical Association. The holotype is stored in the mineralogical collection of the Université Catholique de Louvain, Louvain-la-Neuve, Belgium, under catalog number P1284.

EXPERIMENTAL METHODS

A MAC-5 electron microprobe was used in the energy-dispersion (ED) mode for chemical analysis. The following standards were used: cassiterite (Sn$L\alpha$), PbTe (Pb$M\alpha$), manganotantalite (Mn$K\alpha$, Ta$M\alpha$), $CaNb_2O_6$ (Ca$K\alpha$, Nb$L\alpha$), $CoNb_2O_6$ (Nb$L\alpha$), chromite (Fe$K\alpha$), titanite (Ti$K\alpha$), stibiotantalite (Sb$L\alpha$), microlite (Na$K\alpha$, Ca$K\alpha$). Analyses were carried out at 15 kV accelerating potential, 6 nA sample current measured on fayalite, and 200 s (live) count time. The spectra were collected with a KEVEX model 7000 ED spectrometer and were reduced with KEVEX software using the program MAGIC V (Colby 1980). Peak overlaps were resolved by stripping techniques using library spectra derived from microprobe standards with matrices similar to those of the individual samples. Where apparently excessive cation sums resulted, enough Fe^{2+} to Fe^{3+} (in the columbite-like minerals) or Sn^{2+} to Sn^{4+} (in foordite-thoreaulite phases) was converted to reduce the cation sum to its ideal value.

Unit-cell dimensions were refined from diffractograms obtained on a Philips apparatus using monochromated Fe$K\alpha$ radiation (λ 1.9373 Å), scanning speed ½° 2θ/min and Pb(NO$_3$)$_2$ as an internal standard (a 7.8568 Å). In the case of type foordite, unit-cell parameters for the fragment used for structure analysis were refined using a Nicolet $R3m$ single-crystal four-circle diffractometer with graphite-monochromated Mo$K\alpha$ radiation.

The density was calculated from the unit-cell volume and content, based on X-ray-diffraction data and chemical composition, respectively. The mean index of refraction was calculated using the specific molar refractivities of Mandarino (1981).

FOORDITE

The holotype foordite described here comes from about 15 km NNW of Lutsiro, along the Sebeya River in western Rwanda. The holotype is the same specimen as that examined by Thoreau *et al.* (1950). It was found as a 30-g subangular pebble in alluvial

deposits of the Sebeya basin. Although the primary locality of the specimen is not known, the parent rock can be safely assumed to be a granitic pegmatite. Foordite constitutes about half of the specimen, the other half being predominantly ferrocolumbite and other associated minerals as described below.

Physical properties

The physical properties of type foordite, summarized in Table 1, are close to those of thoreaulite. Optical properties were checked only qualitatively because of the impurity of the material. Orientation of the cleavages was assigned by analogy to thoreaulite. The agreement between the measured and calculated densities is surprisingly good, considering the extensive contamination of foordite by veins and inclusions of other minerals.

Chemical composition

Table 2 shows the chemical composition of the foordite fragment that was used for the crystal-structure analysis (cf. Ercit & Černý 1988). The composition can be taken as representative of the type foordite, being close to the average of other data sets, whose range also is shown in the Table. The chemical composition gives a perfectly stoichiometric formula $(Sn^{2+}_{0.87}Pb_{0.13})_{\Sigma1.00}(Nb_{1.40}Ta_{0.60})_{\Sigma2.00}O_6$ if all Sn is considered to be divalent. Inverse relationships are observed in the Sn vs. Pb ($R = -0.96$ on 11 points) and Nb vs. Ta data, indicating some variability in the populations of both cation sites.

Crystallography

The symmetry, unit-cell dimensions, space group, and X-ray powder-diffraction data of foordite are closely comparable to those of thoreaulite (Nekrasov et al. 1982), synthetic $SnNb_2O_6$ and synthetic $SnTa_2O_6$ (Bodiot 1968). Table 1 summarizes the principal crystallographic characteristics; the justification of the space group $C2/c$ is given in Ercit & Černý (1988). Table 3 gives the X-ray powder-diffraction pattern of the type foordite and of the Maniéma thoreaulite. The latter is an improvement upon PDF 23–596, in which several diffraction maxima are misindexed.

Associated minerals

In their 1950 study of the Lutsiro mineral, Thoreau et al. (1950) recognized columbite and thoreaulite as the main components of the specimen, and they also identified cassiterite by its properties in reflected light. They also described the complex textural relationships of these minerals; replacement of thoreaulite by columbite was proposed, and an exsolution

TABLE 1. PHYSICAL PROPERTIES AND CRYSTALLOGRAPHY
OF THE LUTSIRO FOORDITE

Lustre	vitreous to adamantine	Density (meas.)*	6.734 g/cm³
Color	brownish yellow with	Density (calc.)	6.664 g/cm³
	a greenish tint	α,β,γ	>1.780
Streak	yellowish white	$(\alpha,\beta,\gamma)/3$ (calc.)	2.294
Hardness	6	2V (est.) (+), intermediate
Cleavage	{100} perfect,	$\gamma-\alpha$ (est.)	>0.100
	{011} poor		

| Monoclinic | | Point group | 2/m |
| $SnNb_2O_6$, Z=4 | | Space group | C2/c |

	single-crystal**	powder data**
a, Å	17.093(3)	17.097(2)
b	4.877(1)	4.879(1)
c	5.558(1)	5.562(1)
β, °	90.85(1)	90.85(2)
V, Å³	463.3(1)	463.9(1)

$a:b:c$ (from unit-cell dimensions) 3.504:1:1.140

* from Thoreau et al. (1950)
** see text for experimental conditions

TABLE 2. CHEMICAL COMPOSITION OF THE LUTSIRO FOORDITE*

	representative wt. %	range wt.%	cation contents based on 6 oxygens
SnO	25.4	24.6-26.1	0.87 } 1.00
PbO	6.0	5.3-6.6	0.13 }
Ta_2O_5	28.7	27.0-30.9	0.60 } 2.00
Nb_2O_5	40.1	36.5-40.7	1.40 }
	100.2		

* see text for experimental conditions

TABLE 3. X-RAY POWDER-DIFFRACTION DATA*

	FOORDITE, Lutsiro (THF-5)			THOREAULITE, Maniéma (THF-1)		
hkl	$d_{obs.}$(Å)	$d_{calc.}$(Å)	I/I_0	$d_{obs.}$(Å)	$d_{calc.}$(Å)	I/I_0
200	8.541	8.548	15	8.586	8.571	15
110	4.695	4.691	<5	4.687	4.682	<1
400	4.270	4.274	5	4.281	4.286	<5
11$\bar{1}$	3.592	3.593	40	3.574	3.571	10
31$\bar{1}$	3.100	3.098	50	3.098	3.096	35
311	3.071	3.071	50	3.070	3.067	40
600	2.849	2.849	100	2.860	2.857	100
002	2.781	2.781	20	2.777	2.775	10
20$\bar{2}$	2.654	2.656	5	2.653	2.653	5
202	2.636	2.633	15	2.629	2.628	10
51$\bar{1}$	2.513	2.513	<5	2.515	2.515	5
511	2.489	2.489	10	2.487	2.489	<5
020	2.439	2.439	20	2.434	2.434	10
40$\bar{2}$	2.347	2.347	10	2.346	2.347	5
31$\bar{2}$	2.235	2.235	5	2.234	2.232	<5
710	2.183	2.184	5	2.187	2.188	<5
800	2.137	2.137	5	2.143	2.143	10
71$\bar{1}$	2.043	2.042	10	2.044	2.045	5
711	2.023	2.024	<5	2.025	2.025	5
60$\bar{2}$	2.005	2.005	10	2.007	2.007	5
602	1.975	1.975	10	1.974	1.975	10
620	1.853	1.853	30	1.853	1.853	20
022	1.834	1.834	20	1.830	1.830	10
22$\bar{2}$	1.796	1.797	5	1.793	1.793	5
222	1.789	1.789	15	1.785	1.786	10
11$\bar{3}$	1.727	1.726	15	1.723	1.723	10
80$\bar{2}$	1.707	1.707	<5	1.710	1.709	5
91$\bar{1}$	1.694	{ 1.694	45	1.697	1.697	20
422		1.691		1.691	1.689	10
802	1.681	{ 1.682	45	1.683	{ 1.683	25
911		1.680			1.682	
31$\bar{3}$	1.664	1.664	<5	--	--	--
313	1.652	1.651	<5	--	--	--
62$\bar{2}$	1.549	1.549	10	1.548	1.548	5
513	1.535	{ 1.537	20	1.533	{ 1.535	10
622		1.535			1.533	
33$\bar{1}$	1.507	1.507	10	1.504	1.504	5
331	1.504	1.504	15	1.501	1.501	10

* see text for experimental conditions, and Table 7 for unit-cell dimensions used for calculating d-values.

TABLE 4. MINERALS ASSOCIATED WITH THE LUTSIRO FOORDITE[1]

Assemblages bordering or veining foordite

   (*i*) stannoan plumbomicrolite + cassiterite + ferrocolumbite*
   (*ii*) cassiterite + ixiolite + ferrocolumbite

Associations constituting the foordite-free material

   (*iii*) coarse Ta-rich cassiterite + fine-grained ferrocolumbite
   (*iv*) ferrocolumbite matrix + vermicular "staringite" (±ixiolite)
   (*v*) **ferrocolumbite + ferrotantalite (±plumboan microlite)
   (*vi*) **ferrocolumbite + Ta-poor cassiterite
   (*vii*) ** ferrocolumbite of variable composition

[1] See Table 5 for typical compositions of the different minerals.
* All columbites-tantalites and ixiolites are slightly (~1%) to
  considerably (5%) deficient in (Fe,Mn).
** Local microscopic blebs (<0.05 mm across) with average grain
  size of about 0.008 mm.

intergrowth of vermicular cassiterite in a tantalite matrix was observed.

Examination of the type specimen using the electron microprobe showed a greater diversity of minerals, some of which have considerable compositional ranges. Two types of mineral assemblages can be distinguished: those that are in contact with, or vein, foordite, and those that constitute the columbite-dominated, foordite-free part of the specimen. The mineral assemblages are listed in Table 4, and chemical compositions typical of the different minerals are shown in Table 5.

Because of the extremely fine-grained nature of the complex intergrowth, most mineral names are based only on a chemical composition and optical properties, as they could not be verified by X-ray-diffraction methods. For example, the phase designated ixiolite could conceivably possess an ordered wodginite structure; however, this structure has not yet been found for such a Nb–Fe-dominant composition (Ercit *et al.* 1984, Ercit 1986, Wise & Černý 1986).

The complexity of the mineral assemblages shown in Table 4 suggests that the assemblages represent either several stages of crystallization, or a simultaneous growth of metastable phases; alternatively, a combination of both these processes may have generated a complex disequilibrium assemblage. Textural relationships suggest that the third possibility is the most probable: foordite, stannoan plumbomicrolite and coarse cassiterite seem to be the earliest phases, replaced by ferrocolumbite plus cassiterite, or ixiolite, which largely broke down to "staringite" (Burke *et al.* 1969) plus ferrocolumbite or Ta-poor cassiterite plus ferrocolumbite. The composition of the ferrocolumbite, considerably heterogeneous at a scale of less than 0.05 mm, and its local association with ferrotantalite suggest rapid, disequilibrium nucleation and a lack of subsequent recrystallization. The textural relationships suggesting replacement of foordite by ferrocolumbite and ixiolite are supported by the Ta/(Ta+Nb) values of the metasomatic phases, which are close to that of the foordite, ~0.30.

THE FOORDITE–THOREAULITE SERIES

Samples examined

Table 6 lists the specimens of foordite and thoreaulite examined in the present study. Of the seven known occurrences of these minerals, specimens were available from all localities except the two from the U.S.S.R.: Ungursai in eastern Kazakhstan (Barsanov & Ginsburg 1946, Voloshin *et al.* 1983) and "one of the ore districts of Siberia" (Nekrasov et al. 1982, 1984). Thoreaulite from both of these occurrences, however, has Ta/(Ta + Nb) in the range of 0.56 to 0.66, which is represented in our data set by THF–12 and THF–6, respectively.

Chemical composition

Table 7 shows the chemical composition, unit-cell dimensions, calculated density and calculated mean index of refraction for the available specimens. Several conclusions may be derived from these data:

(*i*) In terms of the Ta/(Ta + Nb) ratio, the analyzed specimens range from 0.30 to 0.91, covering 61% of the total range. Despite the relative scarcity of data, no rational miscibility gaps are suggested (as indicated by XRD data on synthetic end-members and by the crystal-structure refinements; Bodiot 1968, Ercit & Černý 1988). The lack of compositions in the lowermost 30% of the Ta/(Ta + Nb) range is caused by geochemical restrictions on foordite occurrences rather than crystal-chemical constraints (*cf.* "Concluding Remarks" below).

(*ii*) In addition to the Lutsiro holotype of foordite, the "thoreaulite" from Kubitaka, Punia also was found to have Ta/(Ta + Nb) less than 0.5 and should be designated as foordite. A slight dominance of Nb over Ta, indicated for this occurrence in the original analysis by Thoreau *et al.* (1950), was confirmed here for the original specimen (Table 7, THF–3). Another specimen from Punia, THF–7, has a Ta/(Ta + Nb) value very close to that of the Lutsiro mineral and can be designated a cotype.

(*iii*) With reliable standards and data-reduction procedures for the electron-microprobe analyses (which were proven to give excellent results for other Nb–Ta–Sn-rich oxide minerals; Ercit 1986), the totals (wt.% and atomic contents) for the foordite-thoreaulite series come close to the ideal 100% and 12 cations per 24 oxygen atoms, respectively, if all Sn is calculated as SnO. In contrast, considerable, persistent and internally consistent deviations from these values result if the Sn content is expressed as SnO_2 (101.5 to 103.2 wt.% totals, 10.1 to 10.5 cations per 24 oxygen atoms). However, a perceptible improvement in the cation totals of the individual sites is achieved in 7 of 11 analyses by normalizing the unit-cell contents to 12 cations and 24

TABLE 5. CHEMICAL COMPOSITION OF MINERALS ASSOCIATED WITH THE LUTSIRO FOORDITE

	(i)*			(ii)			(iii)		(iv)				(v)			(vi)		(vii)	
	fc	cass	mic	ix	fc	cass	cass	cass	ix	fc	star	star	fc	ft	mic	fc	cass	fc	fc
Ta_2O_5	25.7	4.0	50.1	21.7	32.6	4.8	7.9	1.3	36.5	36.9	20.3	25.2	34.9	56.0	64.1	44.4	1.3	34.7	46.9
Nb_2O_5	56.1	0.8	11.3	47.5	49.0	0.7	3.6		40.3	45.6	20.4	24.8	47.1	28.4	13.4	39.5	0.2	47.6	36.7
SnO_2	0.4	95.1		14.7		92.9	85.5	98.5	7.3	0.9	51.1	39.9	0.4	0.2		0.5	98.3		0.3
SnO			12.9																
PbO			22.4												11.3				
FeO	16.0	0.8	1.4	13.2	14.3	1.1	1.9		13.4	14.6	7.3	9.1	14.9	13.4	2.3	14.1	0.4	15.0	13.9
MnO	2.7			2.9	3.5		0.5		2.3	2.6	1.3	1.5	2.6	2.4	0.3			2.8	2.4
CaO															2.6				
Na_2O			0.9												1.9				
Sum	100.9	100.7	99.0	100.0	99.4	99.5	99.4	99.8	99.8	100.6	100.4	100.5	99.9	100.4	95.9	100.8	100.2	100.1	100.2
Ta	1.73	0.054	11.64	1.51	2.30	0.066	0.108	0.018	2.67	2.63	0.78	0.96	2.48	4.37	11.87	3.26	0.018	2.45	3.51
Nb	6.28	0.018	4.36	5.50	5.75	0.016	0.082		4.90	5.39	1.31	1.57	5.56	3.69	4.13	4.82	0.005	5.60	4.56
Sn^{4+}	0.04	1.893		1.50		1.874	1.712	1.978	0.78	0.09	2.88	2.22	0.04	0.02		0.05	1.964		0.03
Sn^{2+}			4.91												2.07				
Pb			5.15																
Fe	3.32	0.033	1.00	2.83	3.10	0.047	0.080		3.01	3.19	0.86	1.06	3.25	3.22	1.31	3.18	0.017	3.26	3.20
Mn	0.57			0.63	0.77		0.021		0.52	0.58	0.16	0.18	0.58	0.58	0.17	0.53		0.62	0.56
Ca															1.90				
Na			1.49												2.51				
Sum	11.94	1.998	28.56	11.97	11.92	2.003	2.003	1.996	11.88	11.88	5.99	5.99	11.91	11.88	23.96	11.84	2.004	11.93	11.86

* see Table 4 for the individual assemblages; fc - ferrocolumbite (cell contents on 24 oxygens); ft - ferrotantalite (24 oxygens);
cass - cassiterite (4 oxygens); mic - microlite (16 Ta+Nb); ix - ixiolite (24 oxygens); star - "staringite" (12 oxygens).

oxygen atoms, converting a proportion of the Sn^{2+} to Sn^{4+}, and assigning the latter to the (Nb,Ta) site, as has been done in Table 7. This calculated Sn^{4+} in all cases is lower than 3% of the total Sn content.

We conclude that the electron-microprobe data indicate that the vast majority of Sn in foordite-thoreaulite is in the divalent state. The presence of Sn^{4+}, if any, is restricted to minor quantities that are close to the limits of analytical uncertainty.

(*iv*) Attempts to determine the Sn^{2+}/Sn^{4+} ratio by Mössbauer spectroscopy were abandoned because all specimens at our disposal are contaminated by inseparable replacement-products, including cassiterite. From this viewpoint, the significance of the Mössbauer study of Nekrasov *et al.* (1982), suggestive of ~25% Sn in the Siberian thoreaulite being quadrivalent, seems doubtful. Subsequent study of this material by Nekrasov *et al.* (1984) showed a widespread presence of cassiterite.

(*v*) Nekrasov *et al.* (1982) proposed balancing the Sn^{4+} in the structure of thoreaulite by incorporating additional oxygen over and above the six oxygen atoms in the ideal "Sn^{2+}-only" formula. As shown above (and in Ercit & Černý 1988), this mechanism is ruled out by our results. At present, it is not possible to provide a satisfactory answer. Cation deficiency is a possibility, as is the substitution $^ASn^{2+} + {}^B(Nb,Ta)^{5+} \rightleftharpoons {}^ASb^{3+} + {}^BSn^{4+}$. However, the Sn^{4+} and Sb^{3+} contents are so low in the samples examined that confirmation by quantitative correlation is not possible.

(*vi*) Besides Sn, Nb and Ta, subordinate quanti-

TABLE 6. LIST OF EXAMINED SAMPLES

THF-1 Maniéma, Zaïre (Institut de Minéralogie, Université de Liège, # 2067)
THF-2 Manono, Zaïre (Institut de Minéralogie, Université de Liège, # 2069)
THF-3 Kubitaka, Punia, Zaïre (Institut de Minéralogie, Université de Liège)
THF-4 Gitebi, Lutsiro, Rwanda (Institut de Minéralogie, Université Louvain)
THF-5 Lutsiro, Rwanda (Institut de Minéralogie, Université Louvain, # P1284)
THF-6 Lavra Urubú, Itinga, Minas Gerais, Brazil (J.P. Cassedanne)
THF-7 Punia, Belgian Congo (Department of Mineralogy and Geology, Royal Ontario Museum, # M23809)
THF-8 Manono, Belgian Congo (Department of Mineralogy and Geology, Royal Ontario Museum, #M23809)
THF-9 Zaïre (Department of Mineral Sciences, Smithsonian Institution, U.S. National Museum of Natural History #141844)
THF-10 Manono, Shaba, Zaïre (Department of Mineral Sciences, Smithsonian Institution, U.S. National Museum of Natural History, #106780)
THF-11 Manono, Shaba, Zaïre (Department of Mineral Sciences, Smithsonian Institution, U.S. National Museum of Natural History, # 140361)
THF-12 Lavra Urubú, Itinga, Minas Gerais, Brazil (R.V. Gaines)

ties of Sb and Pb were found in the foordite-thoreaulite minerals. In analogy to the structurally related stibiotantalite, Sb is considered trivalent and is asssigned to the Sn^{2+} site. Pb^{2+} also enters this site, being equivalent to Sn^{2+} in charge and close to it in ionic radius.

Unit-cell dimensions

Unit-cell dimensions listed in Table 7 are plotted against the Ta/(Ta + Nb) value in Figure 1 (except β). Despite some scatter of the data, it is readily apparent that Ta substitution for Nb increases *a* and

TABLE 7. CHEMICAL COMPOSITION OF THE FOORDITE-THOREAULITE MINERALS

	THF-1	THF-2	THF-3	THF-5	THF-6	THF-7	THF-8	THF-9	THF-10	THF-11	THF-12
Ta_2O_5	69.6	69.7	42.7	28.7	53.9	30.9	69.0	66.8	65.2	66.6	48.9
Nb_2O_5	4.6	4.1	28.7	40.1	19.0	40.7	4.7	7.8	8.2	6.8	22.9
SnO_2	0.7	0.4	0.9	0.0	0.0	0.0	0.0	0.1	0.0	0.4	0.2
Sb_2O_3	0.5	1.2	0.3	0.0	0.2	0.0	0.5	0.4	0.8	1.1	0.0
PbO	2.7	2.8	0.5	6.0	1.1	0.7	3.0	0.0	4.1	3.3	1.7
SnO	21.7	21.1	27.1	25.4	24.8	29.5	21.2	24.2	20.6	21.2	25.5
	99.8	99.3	100.2	100.2	99.0	101.8	98.4	99.3	98.9	99.4	99.2
Ta	7.11	7.20	3.73	2.41	5.06	2.51	7.17	6.67	6.62	6.76	4.49
Nb	0.78	0.70	4.17	5.60	2.96	5.49	0.81	1.30	1.37	1.14	3.49
Sn^{4+}	0.11	0.06	0.12	0.00	0.00	0.00	0.00	0.02	0.00	0.06	0.03
ΣB	8.00	7.96	8.02	8.01	8.02	8.00	7.98	7.99	7.99	7.96	8.01
Sb	0.08	0.18	0.04	0.00	0.03	0.00	0.09	0.05	0.12	0.17	0.00
Pb	0.27	0.29	0.04	0.50	0.10	0.06	0.31	0.00	0.41	0.33	0.15
Sn^{2+}	3.64	3.57	3.89	3.49	3.81	3.93	3.62	3.96	3.43	3.54	3.84
ΣA	3.99	4.04	3.97	3.99	3.94	3.99	4.02	4.01	3.96	4.04	3.99
$\Sigma(A,B)$	11.99	12.00	12.01	12.00	11.96	11.99	12.00	12.00	11.95	12.00	12.00
Ta/(Ta+Nb)	0.90	0.91	0.47	0.30	0.63	0.31	0.90	0.84	0.83	0.86	0.56
Density*	8.08	8.12	6.95	6.66	7.36	6.55	8.10	7.89	7.95	7.80	7.21
$(\alpha+\beta+\gamma)/3$*	2.243	2.238	2.261	2.293	2.255	2.274	2.248	2.245	2.256	2.252	2.261
a, Å	17.145(2)	17.148(3)	17.101(3)	17.097(2)	17.115(3)	17.090(3)	17.144(3)	17.124(2)	17.145(3)	17.142(3)	17.107(2)
b, Å	4.867(1)	4.867(1)	4.872(1)	4.879(1)	4.870(1)	4.875(1)	4.868(1)	4.869(1)	4.864(1)	4.867(1)	4.873(1)
c, Å	5.551(1)	5.551(1)	5.556(1)	5.562(1)	5.554(1)	5.562(1)	5.551(1)	5.552(1)	5.552(1)	5.552(1)	5.554(1)
β, °	90.92(1)	90.90(1)	90.93(1)	90.85(1)	90.90(1)	90.92(1)	90.88(1)	90.92(1)	90.90(1)	90.90(1)	90.88(1)
V, Å³	463.1(1)	463.2(1)	462.9(1)	463.9(1)	462.9(1)	463.3(1)	463.2(1)	462.9(1)	462.9(1)	463.1(1)	462.9(1)

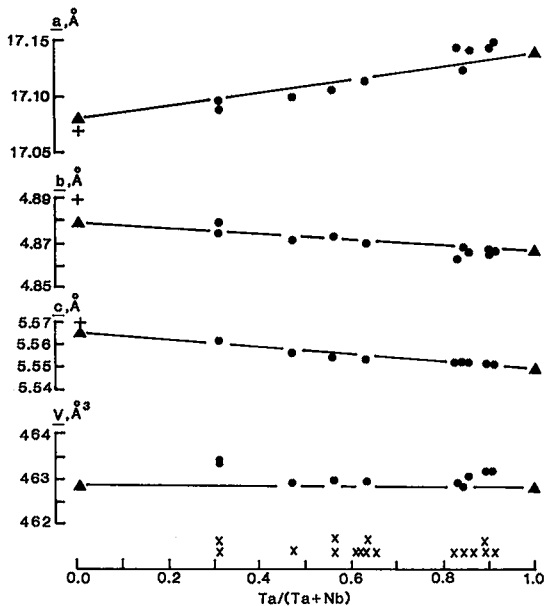*calculated values, see text for procedures

FIG. 1. Unit-cell dimensions *vs.* the Ta/(Ta+Nb) values (atomic) in members of the foordite–thoreaulite series. Symbols: X values for all specimens analyzed in the present study and reported in the recent literature (electron-microprobe data only); + unit-cell dimensions of synthetic $SnNb_2O_6$ (Bodiot 1968); ▲ end-member values extrapolated from the measured data (•), assuming linearity.

decreases b and c, but variation in V is restricted and erratic. Multiple linear-regression analysis shows that Pb^{2+} substitution for Sn^{2+} increases a and decreases c, but has no significant effect on b. Substitution of Sb^{3+} for Sn^{2+} increases a and c, but decreases b. The following regression-equations express Ta, Pb and Sb in fractions of their unit-cell contents:

$$A_o(\text{Å}) = 17.060 + 0.0098(\text{Ta}) + 0.025(\text{Pb}) + 0.06(\text{Sb})$$
$$(R^2 = 98\%; \text{ RMS error in } A_o = 0.003)$$

$$B_o(\text{Å}) = 4.879 - 0.0015(\text{Ta}) + 0.015(\text{Sb})$$
$$(R^2 = 87\%; \text{ RMS error in } B_0 = 0.002)$$

$$C_o(\text{Å}) = 5.565 - 0.0020(\text{Ta}) + 0.011(\text{Sb}) - 0.003(\text{Pb})$$
$$(R^2 = 91\%; \text{ RMS error in } C_o = 0.001)$$

The cell-edge a varies linearly with composition, and the scatter of data is low (Fig. 2A). The same is true of b; the relative variation in this parameter is ~ ⅔ of that in a, thus a greater apparent scatter and lower correlation-coefficient should be expected
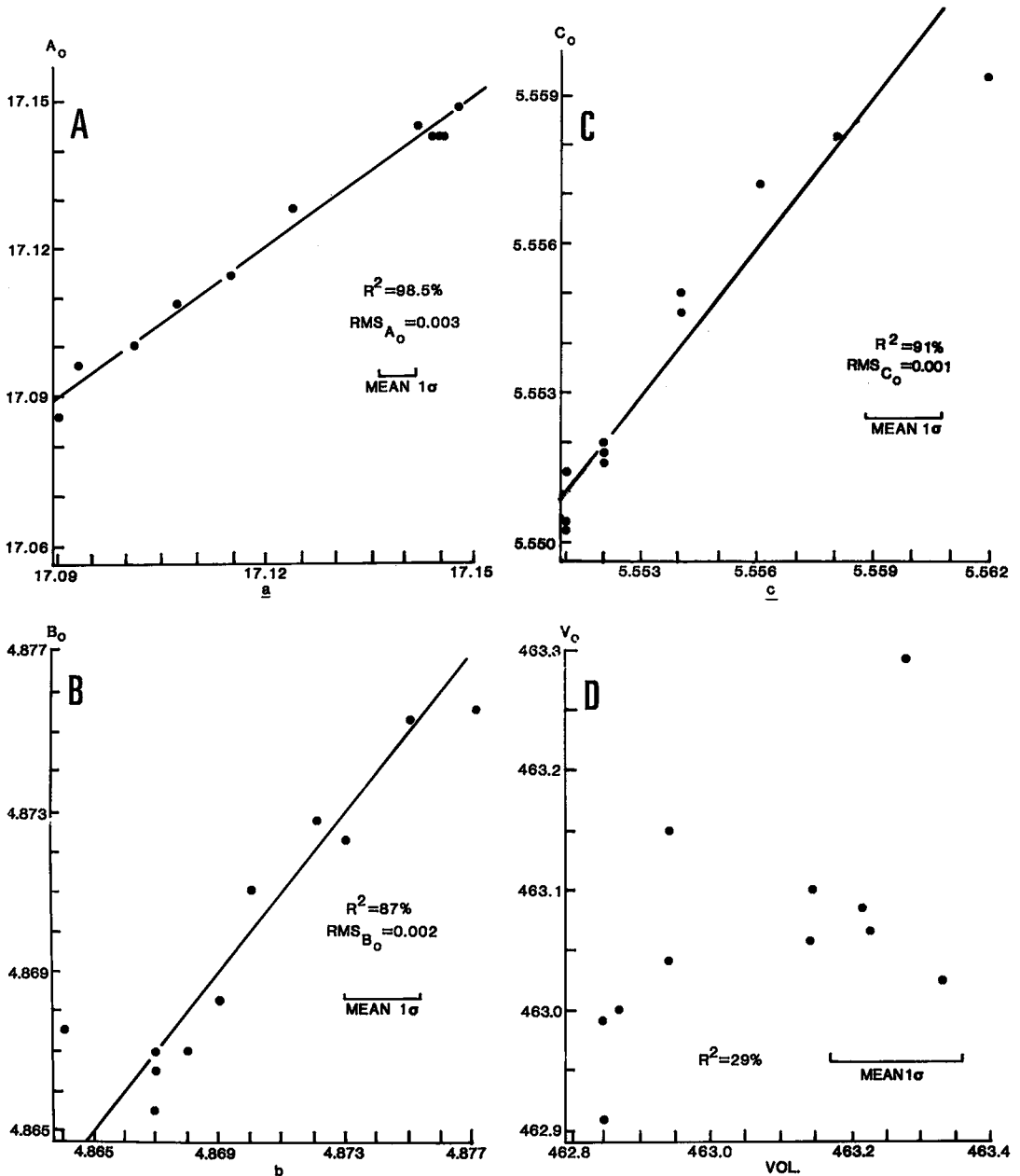
FIG. 2. Multiple-regression fits (curves) to unit-cell dimensions in the foordite–thoreaulite series. See text for equations and specific comments.

(Fig. 2B). The data of Figure 2C suggest an apparent curvilinear trend for c; however, it is not significant: the relative variation in c is less than that in a or b (only $\sim \frac{1}{2}$ of that in a), yet the relative precision of c is poorer than that of a.

The relative variation in V is too slight to permit any analysis of its possible trend; the total variation

in V is only 4.5 times larger than individual, measured standard deviations in V (Fig. 2D). The present data indicate that the compositional variations have no significant effect on V; the difference of 0.3 Å^3 between the extrapolated end-member values amounts to only 0.065% of the higher value.

The β angle is virtually constant throughout the
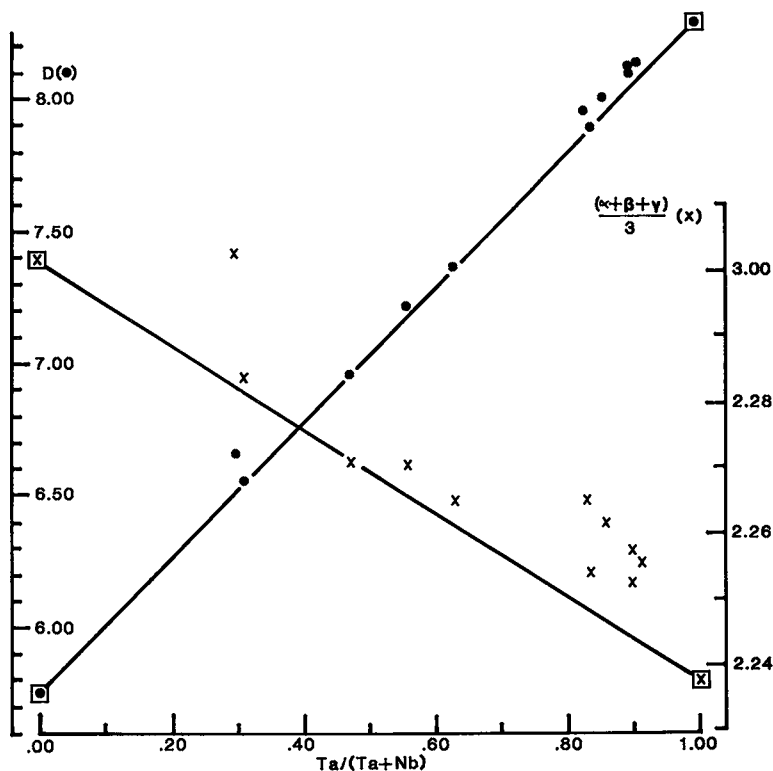
FIG. 3. Multiple-regression fits (curves) to the density (calc.) and the mean index of refraction $(\alpha + \beta + \gamma)/3$ (calc.) in the foordite–thoreaulite series. See text for equations. Substitution of Pb for Sn is mainly responsible for deviation of natural samples from the properties of pure $Sn(Nb,Ta)_2O_6$ compounds.

foordite–thoreaulite series; none of the measured values deviate from the mean by more than 2σ (Table 7). Consequently, the mean value of β was assigned to the end-member compositions.

It should be noted that complete substitution at a structural site of a simple monoclinic compound rarely generates perceptible changes in unit-cell edges without affecting β or V. Foordite–thoreaulite is anomalous in that changes in geometry of the B-site octahedron generated by Nb–Ta substitution are absorbed in the overall structure by dimensional adjustments alone.

Density and mean index of refraction

Multiple regression analysis of values of density D calculated from the chemical composition and unit-cell dimensions leads to the equation:

$$D = 5.75 + 0.317(Ta) + 0.27(Pb) + 0.01\,(Sb),$$

in which the values of Ta, Pb and Sb represent frac-

tions of their unit-cell contents. In a similar way, analysis of mean index of refraction $\bar{n}$ calculated from the chemical composition and density gives the regression equation:

$$(\alpha + \beta + \gamma)/3 = 2.288 - 0.0069(Ta) + 0.040(Pb) - 0.04(Sb)$$

Thus the calculated D and $\bar{n}$ of foordite are 5.75 g/cm^3 and 2.288, respectively, whereas those of thoreaulite are substantially different, as expected from the Nb–Ta substitution: 8.27 g/cm^3 and 2.228. Correlation coefficients and standard errors are not reported for the above equations because in both cases all values are calculated from, and fitted to, compositional data. However, Figure 3 shows the calculated D and $\bar{n}$ values, as well as the regressed curves, plotted against Ta/(Ta+Nb); the graph demonstrates the relative insensitivity of density to the Pb substitution, which considerably disturbs the indices of refraction.

CONCLUDING REMARKS

Two factors contribute to the scarcity of natural occurrences of the foordite–thoreaulite minerals. The parent environment not only must be reducing enough to crystallize a Sn^{2+}-bearing compound, but it also must have low chemical potentials of Fe, Mn, Na, Ca and F.

Cassiterite is the most common Sb-bearing mineral in granitophile parageneses. It is considered to be precipitated in response to changing redox conditions and pH from hydrous Cl- and F-bearing media, in which tin is transported mainly in the divalent state (Eadington 1985). Consequently, conditions leading to crystallization of Sn^{2+}-bearing phases are undoubtedly exceptional, involving not only substantial changes in pH (P?, T?), but also with $f(O_2)$ dropping below the Ni–NiO buffer values. Such a range of oxygen fugacities is close to the Sn^{2+}–Sn^{4+} reaction at a pH corresponding to orthoclase-muscovite equilibrium (Eadington 1985). Besides the foordite–thoreaulite minerals themselves, stannomicrolite is the only other pegmatite mineral with substantial Sn^{2+}. It is known from only a single locality (Vorma & Siivola 1967, Ercit et al. 1987), and it is not surprising that the only other Sn^{2+}-rich microlite encountered to date is the stannoan plumbomicrolite associated with the Lutsiro foordite. The rarity of stannomicrolite, and the association of its close "relative" with foordite, emphasize again the exceptionally low $f(O_2)$ required for their origin. Nekrasov et al. (1982) quoted the proximity of graphitic schists as a factor promoting reducing conditions for the Siberian locality of thoreaulite. Unfortunately, the gross geological conditions and immediate mineral assemblages of other foordite–thoreaulite occurrences either are not well understood, or they have not been examined from this viewpoint.

Similarly to the above requirement of exceptional $f(O_2)$, conditions of low $\mu(Fe,Mn)$ or $\mu(Na,Ca,F)$ or both are rarely realized in granitic pegmatites. Columbite–tantalite and related phases, or microlite, are the usual carriers of Nb and Ta. Extreme depletion in all of the above cations, which allows massive precipitation of Nb and Ta in Fe–Mn–Na–Ca–F-free minerals, is encountered only during late stages of consolidation in highly fractionated pegmatites (in the simpsonite paragenesis; Ercit 1986). Thus it is not surprising that most occurrences, particularly the most voluminous occurrences (as at Manono) of the foordite–thoreaulite minerals are restricted to the Ta-rich compositions, indicative of a high degree of fractionation attained by the parent pegmatite. Conditions of low $f(O_2)$, low $\mu(Fe,Mn,$ Na,Ca,F) and low $\mu(Ta/Nb)$ must be due to exceptional circumstances, and foordite will undoubtedly remain a very rare mineral in general, as well as relative to thoreaulite.

It should be stressed that the conditions generating simpsonite and foordite–thoreaulite are transient. In both cases, replacement by (Fe,Mn)- and alkali-bearing minerals is common (Nekrasov et al. 1982, 1984, Voloshin et al. 1983, Černý & Ercit 1985, Ercit 1986). In the case of foordite–thoreaulite, oxidation of Sn^{2+} during the replacement is characteristic, yielding cassiterite and "staringite" along with other metasomatic products. It is noteworthy that some of the ferromanganoan minerals that coprecipitated with or replaced simpsonite or foordite–thoreaulite, are (Fe,Mn)-deficient. This is the case of tantalum-rich wodginite in the Alto do Giz and Tanco occurrences of simpsonite (Ercit & Černý 1982, Ercit 1986) and of the columbite-tantalite minerals that replaced the Lutsiro foordite (Table 5).

REFERENCES

BAILLY, R. (1942): Propriétés optiques de la thoreaulite. Ann. Soc. Géol. Belgique 65, 169–179.

BARSANOV, G.P. & GINSBURG, A.I. (1946): Thoreaulite – tantalate of tin from a locality in the Kalba Range. Dokl. Akad. Nauk SSSR 54, 619-622 (in Russ.).

BODIOT, D. (1968): Comparaison des éléments niobium et tantale d'après les combinaisons formées, dans l'état solide, par leur hémipentoxyde avec les oxydes. Rev. Chim. Minérale 5, 569-607.

BURKE, E.A.J., KIEFT, C., FELIUS, R.O. & ADUSUMILI, M.S. (1969): Staringite, a new Sn–Ta mineral from north-eastern Brazil. Mineral. Mag. 37, 447-452.

BUTTGENBACH, H. (1933): Minéraux du Congo Belge. Bull. Soc. Géol. Belgique 56, 327-328.

ČERNÝ, P. & ERCIT, T.S. (1985): Some recent advances in the mineralogy and geochemistry of Nb and Ta in rare-element granitic pegmatites. Bull. Minéral. 108, 499-532.

COLBY, J.W. (1980): MAGIC V – a computer program for quantitative electron-excited energy dispersive analysis. *In* QUANTEX-Ray Instruction Manual. Kevex Corporation, Foster City.

EADINGTON, P.J. (1985): The solubility of cassiterite in hydrothermal solutions in relation to some lithological and mineral associations in tin ores. *In* Granite-Related Mineral Deposits, Geology, Petrology and Tectonic Setting (R.P. Taylor & D.F. Strong, eds.). *Can. Inst. Mining Metall., Conf. (Halifax 1985), Extended Abstr.*, 110-115.

ERCIT, T.S. (1986): *The Simpsonite Paragenesis: the Crystal-Chemistry and Geochemistry of Extreme Ta Fractionation.* Ph.D. thesis, Univ. of Manitoba, Winnipeg, Manitoba.

_____ & ČERNÝ, P. (1982): The paragenesis of simpsonite. *Geol. Assoc. Can. - Mineral. Assoc. Can., Prog. Abstr.* **7**, 48.

_____ & _____ (1988): The crystal structure of foordite. *Can. Mineral.* **26**, 899-903.

_____, _____ & HAWTHORNE, F.C. (1984): The crystal chemistry of wodginite. *Geol. Soc. Amer., Abstr. Prog.* **16**, 502.

_____, _____ & SIIVOLA, J. (1987): The composition of stannomicrolite. *Neues Jahrb. Mineral. Monatsh.*, 249-252.

FOORD, E.E. (1982): Minerals of tin, titanium, niobium and tantalum in granitic pegmatites. *In* Granitic Pegmatites in Research and Industry (P. Černý, ed.). *Mineral. Assoc. Can., Short Course Handbook* **8**, 187-238.

GORZHEVSKAYA, S.A. & SIDORENKO, G.A. (1974): On crystallochemical properties of the columbite-ixiolite–wodginite series. *Constit. Prop. Mineral.* **8**, 30-36 (in Russ.).

GRAHAM, J. & THORNBER, M.R. (1974): The crystal chemistry of complex niobium and tantalum oxides. 1. Structural classification of MO_2 phases. *Amer. Mineral.* **59**, 1026-1039.

KHVOSTOVA, V.A., SLESARCHUK, V.S. & LAPUTINA, I.P. (1974): First find of staringite in the Soviet Union. *Trudy Mineral. Muzeya Akad. Sci. SSSR* **23**, 226-228 (in Russ.).

MAKSIMOVA, N.V. & ILYUKHIN, V.V. (1967): On the crystal structure of thoreaulite $Sn(Ta,Nb)_2O_7$. *Sov. Phys. Cryst.* **1**, 105-106.

_____, _____ & BELOV, N.V. (1975): Crystal structure of thoreaulite $SnTa_2O_6$. *Dokl. Akad. Nauk SSSR* **223**, 1115-1118 (in Russ.).

MANDARINO, J.A. (1981): The Gladstone–Dale relationship. IV. The compatibility concept and its application. *Can. Mineral.* **19**, 441-450.

MÉLON, J. (1935): Analyse et propriétés optiques de la thoreaulite. *Bull. Acad. Roy. Belgique (Cl. Sci.)* **4**, 473-475.

_____ & TOUSSAINT, J. (1950): La thoreaulite de Kubitaka (Punia, Maniéma, Congo Belge) et la cristallographie de la thoreaulite. *Ann. Soc. Géol. Belgique* **74**, B25-B32.

MUMME, W.G. (1970): The crystal structure of thoreaulite, $SnTa_2O_7$, an example of tin in five-fold coordination. *Amer. Mineral.* **55**, 367-377.

NEKRASOV, I.YA., CHISTYAKOVA, N.I. & YEVSTIGNEYEVA, T.L. (1984): On the relationships of thoreaulite, lithiotantite, rankamaite and cassiterite in rare-element pegmatites of Siberia. *Mineral. Zh.* **6**, 42-55 (in Russ.).

_____, NEKRASOVA, R.A., TSEPIN, A.I., SIPAVINA, L.V. & REMEZ, V.K. (1982): Thoreaulite from rare-metal pegmatite of Siberia. *Mineral. Zh.* **4**, 11-20 (in Russ.).

THOREAU, J., GASTELLIER, S. & HERMAN, P. (1950): Sur une thoreaulite du Ruanda Occidental. *Ann. Soc. Géol. Belgique* **73**, B213-B220.

VOLOSHIN, A.V., PAKHOMOVSKY, YA. A., STEPANOV, V.I. & TYUSHEVA, F.N. (1983): Lithiotantite $Li(Ta,Nb)_3O_8$ – a new mineral from granitic pegmatites of eastern Kazakhstan. *Mineral. Zh.* **5**, 91-95 (in Russ.).

VORMA, A. & SIIVOLA, J. (1967): Sukulaite – $Ta_2Sn_2O_7$ – and wodginite as inclusions in cassiterite in the granite pegmatite in Sukula, Tammela in SW Finland. *Comptes Rend. Soc. Géol. Finlande* **39**, 173-187.

WISE, M.A. & ČERNÝ, P. (1986): The status of ixiolite. *Int. Mineral. Assoc., 14th Gen. Meet. (Stanford 1986), Abstr. Progr.*, 265.